Pillar[5]arene-porphyrin conjugates: from molecular flowers to photoactive rotaxanes

Iwona Nierengarten, Uwe Hahn, Michel Holler, Béatrice Delavaux-Nicot, Emmanuel Maisonhaute, Jean-François Nierengarten

Pillar[5]arene-porphyrin conjugates: from molecular flowers to photoactive rotaxanes

Iwona Nierengarten[a], Uwe Hahn[a], Michel Holler[a], Béatrice Delavaux-Nicot[b], Emmanuel Maisonhaute[c] and Jean-François Nierengarten[*a]

[a] *Laboratoire de Chimie des Matériaux Moléculaires, Université de Strasbourg et CNRS (UMR 7042, LIMA), Ecole Européenne de Chimie, Polymères et Matériaux (ECPM), 25 rue Becquerel, 67087 Strasbourg Cedex 2, France*

[b] *Laboratoire de Chimie de Coordination du CNRS (UPR 8241), Université de Toulouse (UPS), 205 Route de Narbonne, BP 44099, 31077 Toulouse Cedex 4, France*

[c] *Sorbonne Université, CNRS, Laboratoire Interfaces et Systèmes Electrochimiques, 4 Place Jussieu, 75005 Paris, France*

Dedicated to Prof. Tomás Torres on the occasion of his 70th birthday

Received date (to be automatically inserted after your manuscript is submitted)
Accepted date (to be automatically inserted after your manuscript is accepted)

ABSTRACT: Our groups are involved in a research program on the development of molecular and supramolecular systems combining pillar[5]arene building blocks with porphyrins. Functionalization of both rims of the pillar[5]arene scaffold with metalloporphyrins generated giant molecular machines mimicking the blooming of a flower as well as light harvesting devices. On the other hand, we have also used the host-guest properties of pillar[5]arene derivatives to prepare photoactive mechanically interlocked molecules. In such compounds, complementary subunits are associated into a single molecular ensemble but without being connected through covalent bonds. Inter-component photo-induced energy transfer processes remain however extremely fast in these systems despite the exclusive link through mechanical bonds. All these results are described in the present review.

KEYWORDS: Porphyrin, pillar[5]arene, rotaxane, molecular flower, photoactive molecular devices

*Correspondence to: Jean-François Nierengarten, email: nierengarten@unistra.fr

INTRODUCTION

Pillar[5]arenes are *para*-cyclophanes composed of five 1,4-disubstituted hydroquinone moieties linked by methylene bridges in their 2,5-positions [1]. These tubular-shaped macrocyclic compounds are efficiently prepared from readily available 1,4-disubstituted benzene derivatives and paraformaldehyde in the presence of a Lewis acid catalyst [2-3]. Following the first example reported in 2008 by T. Ogoshi [3], pillar[5]arenes became rapidly popular macrocyclic building blocks in the field of supramolecular chemistry [1] and their host-guest chemistry has been intensively investigated [4]. Owing to their electron-rich aromatic subunits, pillar[5]arenes are supramolecular receptors for electron-poor molecules such as viologen and imidazole cations [4]. In addition to charge-transfer interactions between the electron-rich cavity of pillar[5]arenes and electron-poor guest molecules, C-H···π interactions play also an important role for the formation of inclusion complexes. Simple alkyl-substituted guests are effectively encapsulated in the pillar[5]arene cavity to form inclusion complexes [4]. A rich variety of supramolecular systems have been reported so far and some found applications in the fields of materials science and biology [5]. As part of this research, our groups took profit of the ten peripheral functional subunits present around the pillar[5]arene scaffold to prepare multifunctional nanomaterials with specific properties [6-10]. Examples include bioactive glycoclusters [6], non-viral gene transfection vectors [7], hole transporting materials for perovskite solar cells [8], electroactive nanomaterials for the preparation of modified electrodes [9] and liquid-crystalline materials [10]. On the other hand, we have also used the host-guest properties of pillar[5]arene derivatives to generate supramolecular nanomaterials [11] and mechanically interlocked molecules, namely rotaxanes [12]. The combination of our pillar[5]arene-containing building blocks with metalloporphyrin derivatives also attracted our attention owing to their specific electronic properties for the preparation of photo- and/or electro-active molecular devices. This latter aspect of our research program on functionalized pillar[5]arene derivatives is summarized in the present account.

RESULTS AND DISCUSSION

Multiporphyrin arrays constructed on a pillar[5]arene scaffold

Owing to their ability to form apical complexes with *N*-ligands, metalloporphyrins are attractive building blocks for the construction of supramolecular systems [13]. Whereas pyridines and imidazoles are typical ligands for such constructions, 1,2,3-triazole derivatives also emerged as potential candidates to coordinate metalloporphyrins [14-16]. 1,2,3-Triazoles are however significantly less basic when compared to pyridines and imidazoles [17]. They are thus weaker ligands. This is illustrated by the binding constant (K_A) of 480 M^{-1} derived for the coordination of 1*H*-1,2,3-triazole to Zn(II)-tetraphenylporphyrin in toluene which is one order of magnitude lower than the K_A value obtained for pyridine under the same conditions (5800 M^{-1}) [15]. The triazole-metalloporphyrin alone is therefore not perfectly suited for the assembly of stable supramolecular nanostructures. It has been however successfully used to self-assemble well-defined macrocyclic nanostructures from bis- and tris-porphyrin building blocks endowed with two triazole moieties [18]. In this case, multiple interactions and cooperative effects ensure the stability of the macrocyclic ensembles. On the other hand, intramolecular triazole-metalloporphyrin interactions have been also observed in multi-Zn(II)-porphyrinic arrays **1Zn$_{10}$** and **2Zn$_{10}$** constructed on a pillar[5]arene scaffold [19]. These compounds and the corresponding free-base derivatives (**1(H$_2$)$_{10}$** and **2(H$_2$)$_{10}$**) are depicted in Figure 1.

Figure 1

For both **1Zn$_{10}$** and **2Zn$_{10}$**, detailed NMR studies revealed dynamic exchange between different conformers. At room temperature, intramolecular coordination interactions between some 1,2,3-triazole linkers and metal centers of neighboring Zn(II)-porphyrin moieties are responsible for a partial folding of compounds **1Zn$_{10}$** and **2Zn$_{10}$** (Figure 2). This view has been further supported by DOSY experiments performed in CD_2Cl_2 at room temperature. Comparison of the free-base porphyrin derivatives with their Zn(II) analogues revealed effectively volume reductions of 32 (**1Zn$_{10}$** vs. **1(H$_2$)$_{10}$**) and 22% (**2Zn$_{10}$** vs. **2(H$_2$)$_{10}$**). The partial coordination of Zn(II)-porphyrin moieties with neighboring 1,2,3-triazole subunits in compounds **1Zn$_{10}$** and **2Zn$_{10}$** has been also supported by their UV/vis spectra. As a typical example, the absorption spectra recorded in different solvents at room temperature for **1Zn$_{10}$** are depicted in Figure 2. The absorption bands of the Zn(II)porphyrin moieties are broadened and red-shifted when compared to those of typical Zn(II)porphyrin derivatives. This is a clear signature for a partial intramolecular apical coordination of Zn(II) cations in **1Zn$_{10}$**. The shape of the absorption spectra of both **1Zn$_{10}$** and **2Zn$_{10}$** is also sensitive to the solvent. Intramolecular coordination in **1Zn$_{10}$** and **2Zn$_{10}$** is actually more favorable in less polar solvents. The intensity of the red-shifted absorption maxima of the Soret band that is typical for coordinated Zn(II)-porphyrins is effectively increased when going from CH_2Cl_2 to PhMe or from $CHCl_3$ to CH_2Cl_2. The absorption spectra of the free-base derivatives **1(H$_2$)$_{10}$** and **2(H$_2$)$_{10}$** are also depicted in Figure 2. In contrast to what was observed for their Zn(II) analogues, the absorption spectra of **1(H$_2$)$_{10}$** and **2(H$_2$)$_{10}$** are only very slightly broadened when compared to a simple free-base porphyrin thus showing rather limited electronic interactions (if any) among the free-base porphyrin moieties in **1(H$_2$)$_{10}$** and **2(H$_2$)$_{10}$**.

Figure 2

The intramolecular coordination interactions between the 1,2,3-triazole linkers and the metal centers of neighboring Zn(II)-porphyrin moieties are rather weak and therefore also temperature sensitive. At 105°C, the intramolecular coordination interactions are totally disrupted and both **1Zn$_{10}$** and **2Zn$_{10}$** adopt a fully open structure similar to the one of their free-base analogues. The ^{1}H NMR spectra recorded for **1-2Zn$_{10}$** and **1-2(H$_2$)$_{10}$** at high temperature in $CDCl_2CDCl_2$ are effectively very similar. In contrast, lowering the temperature favors the association thus leading to the folding of **1Zn$_{10}$** and **2Zn$_{10}$**. Overall the intramolecular coordination process is leading to a folded compact structure at low temperature. This is similar to the case of proteins in which weak H-bonds are responsible of their globular secondary structures. By increasing the temperature, denaturation occurs as the weak intramolecular interactions are disrupted, this effect being fully reversible in the case of compounds **1Zn$_{10}$** and **2Zn$_{10}$**.

By using an external chemical input, it has been possible to disrupt the intramolecular coordination interactions in **1Zn$_{10}$** and **2Zn$_{10}$** and thus trigger the blooming of the molecular flowers (Figure 3). For this purpose, an excess of 1-phenylimidazole has been added to solutions of **1Zn$_{10}$** and **2Zn$_{10}$**. As imidazoles are stronger ligands for Zn(II)porphyrins when compared to 1,2,3-triazoles, preferential intermolecular coordination of the Zn(II) cations in **1Zn$_{10}$** and **2Zn$_{10}$** occurs in the presence of an excess of 1-phenylimidazole. This has been evidenced by the dramatic changes evidenced in the UV/vis spectra of **1Zn$_{10}$** and **2Zn$_{10}$** upon addition of an excess of 1-phenylimidazole. This is shown in Figure 3 for compound **2Zn$_{10}$**. NMR binding studies further confirmed that intermolecular coordination of the Zn(II)porphyrin moieties of **1Zn$_{10}$** and **2Zn$_{10}$** by 1-phenylimidazole is capable of preventing the coordination-induced partial folding of the deca-Zn(II)-porphyrin arrays. This view has been also supported by DOSY experiments. Upon addition of an excess of 1-phenylimidazole to solutions of **1Zn$_{10}$** and **2Zn$_{10}$**, volume expansions of 46 (**1Zn$_{10}$**) and 49% (**2Zn$_{10}$**) have been effectively observed.

Figure 3

Finally, detailed electrochemistry investigations have shown that the degree of folding of both **1Zn$_{10}$** and **2Zn$_{10}$** can be reversibly controlled by an electrochemical input (Figure 4). Compounds **1Zn$_{10}$** and **2Zn$_{10}$** are indeed molecular machines mimicking the blooming of a flower. As already discussed, both compounds adopt a partially folded structure in the neutral state. Upon reduction of their ten peripheral Zn(II)porphyrin subunits, total decoordination occurs thus leading to fully unfolded decaanions. In other words, reduction promotes the complete blooming of the molecular flowers. In contrast, oxidation of the peripheral porphyrins generates totally folded decacations in which all the metal centers of the peripheral Zn(II)porphyrin radical cations are coordinated with a triazole unit.

Figure 4

Multiporphyrinic light harvesting devices

With their ten peripheral Zn(II)porphyrin subunits, **1Zn$_{10}$** and **2Zn$_{10}$** appear as attractive antennae for the design of multichromophoric light harvesting devices [20]. The combination of **1Zn$_{10}$** with an appropriate energy acceptor, namely a free-base porphyrin, has been conveniently achieved by taking advantage of the capability of the pillar[5]arene core to form inclusion complexes allowing for the preparation of rotaxanes. The resulting multichromophoric ensemble (**3Zn$_{10}$(H$_2$)$_1$**) is depicted in Figure 5 together with the corresponding free-base porphyrin model compound (**4H$_2$**).

Figure 5

The ground state absorption spectra of [2]rotaxane **3Zn$_{10}$(H$_2$)$_1$** and model compounds **1Zn$_{10}$** and **4H$_2$** recorded in toluene are shown in Figure 6A. The spectrum of [2]rotaxane **3Zn$_{10}$(H$_2$)$_1$** is dominated by the absorption features of its pillar[5]arene moiety bearing ten peripheral Zn(II)-porphyrin subunits. Typical signatures of the free-base porphyrin unit of its axle component are however clearly detected, in particular in the 500-700 nm region. Absorption maxima corresponding to Q bands of a free-base porphyrin moiety are effectively observed at 517, 591 and 649 nm. The absorption spectrum of **3Zn$_{10}$(H$_2$)$_1$** also coincides within the experimental error with the profile obtained by summation of the spectra of its component subunits, **1Zn$_{10}$** and **4H$_2$**, thus showing the absence of significant ground state interactions of the free-base porphyrin unit with the peripheral Zn(II)-porphyrin moieties.

Figure 6

Emission spectra recorded in toluene for compounds **3Zn$_{10}$(H$_2$)$_1$** and model compounds **1Zn$_{10}$** and **4H$_2$** are also shown in Figure 6. Upon excitation of **3Zn$_{10}$(H$_2$)$_1$** at 425 nm, more than 90% of the light is absorbed by the peripheral Zn(II)-porphyrin moieties. The intensity of the Zn(II)-porphyrin centered fluorescence in **3Zn$_{10}$(H$_2$)$_1$** is however significantly reduced when compared to **1Zn$_{10}$** while, at the same time, the emission arising from the free-base porphyrin moiety is enhanced. Emission spectra of **1Zn$_{10}$** and **3Zn$_{10}$(H$_2$)$_1$** recorded from solutions having the same optical density at the exciting wavelength show that the Zn(II)-porphyrin centered fluorescence is quenched by about 75% in **3Zn$_{10}$(H$_2$)$_1$**. Moreover, the intensity of the free-base-

porphyrin emission is 5 times higher for **3Zn$_{10}$(H$_2$)$_1$** than that of model compound **4H$_2$** when the emission spectra are recorded from solutions having the same concentrations. All these experimental observations are consistent with the occurrence of a Zn(II)-porphyrin → free-base porphyrin singlet energy transfer process [21]. This energy transfer was further supported by the excitation spectra recorded for **3Zn$_{10}$(H$_2$)$_1$**. They are effectively similar to the absorption spectrum of **3Zn$_{10}$(H$_2$)$_1$** thus showing that the free-base porphyrin centered fluorescence is also observed upon excitation of the Zn(II)-porphyrin moieties. The steady-state properties of compounds **3Zn$_{10}$(H$_2$)$_1$** and model compounds **1Zn$_{10}$** and **4H$_2$** have been also investigated in other solvents, namely CH_2Cl_2 and $CHCl_3$. As already discussed for compound **1Zn$_{10}$**, the shape of the absorption spectra of **3Zn$_{10}$(H$_2$)$_1$** is affected by the nature of the solvent and the amount of 1,2,3-triazole units coordinating Zn(II)-porphyrin moieties within **3Zn$_{10}$(H$_2$)$_1$** is not exactly the same in the different solvents. The emission properties of **3Zn$_{10}$(H$_2$)$_1$** in CH_2Cl_2 and $CHCl_3$ are similar to those described in toluene. However, it can be noted that the Zn(II)-porphyrin centered fluorescence in **3Zn$_{10}$(H$_2$)$_1$** is quenched by about 70 and 58% in CH_2Cl_2 and $CHCl_3$, respectively, while a quenching of 75% was observed in toluene. This difference is ascribed to the changes in the coordinated/uncoordinated Zn(II)-porphyrin ratio in **3Zn$_{10}$(H$_2$)$_1$** as a function of the solvent. In toluene, intramolecular coordination is favored and the molecules adopt on average a more folded conformation. As a result the Zn(II)-porphyrins are closer to the free-base porphyrin and the energy transfer is more efficient. In contrast, in $CHCl_3$, the dynamic conformational equilibrium is in favor of a more extended conformation. The average distance between the donor units and the acceptor is thus larger on average and the energy transfer becomes less efficient in this particular solvent.

Photoactive rotaxanes constructed from a fulleropillar[5]arene

As part of this research, we became also interested in the preparation of photoactive rotaxanes combining a porphyrin donor with a fullerene acceptor. For this purpose, one methylene unit of *per*-ethylated pillar[5]arene has been oxidized to generate the corresponding ketone allowing the preparation of a tosylhydrazone to graft the pillar[5]arene moiety onto the fullerene sphere [22]. Compound **5** thus obtained is depicted in Figure 7 together with its X-ray crystal structure. The overall conformation of the pillar[5]arene moiety in **5** is only slightly affected by the presence of the fullerene substituent. The size of its cavity is indeed similar to the one observed in the X-ray crystal structures of parent pillar[5]arene derivatives [3]. As a result, compound **5** retains the ability of pillar[5]arene to form inclusion complexes with guests incorporating long alkyl chains and can be therefore used as a macrocyclic building block for the construction of rotaxanes. This has been demonstrated with the preparation of rotaxanes **6H$_2$** [22] and **7** [23] (Figure 7).

Figure 7

The steady-state properties of rotaxanes **6H$_2$** and **7** have been investigated and compared to those of appropriate model compounds. Despite the exclusive link through mechanical bonds between the different subunits in **6H$_2$** and **7**, the quenching of the stopper emission by the fullerene moiety is efficient in both cases. The porphyrin fluorescence intensity of **6H$_2$** is quenched by about 90% when compared to model compound **4H$_2$**. The lifetime is accordingly reduced from 10.1 to 1.6 ns corresponding to a quenching rate of 6.3×10^8 s^{-1}. The free-base porphyrin singlet excited state is most likely quenched by an initial energy transfer to populate the first fullerene excited state [24]. Under our experimental conditions, it was however not possible to demonstrate whether this initial energy transfer is followed or not by an electron transfer. Indeed, fullerene emission could not be monitored as the residual porphyrin emission is much more intense when compared to the weak

fullerene emission (Φ_{em} < 0.0001). On the other hand, a dramatic quenching of the bodipy fluorescence has been also evidenced in the case of compound **7**. Comparison of the emission intensity of **7** with a model Bodipy rotaxane lacking the C_{60} unit revealed that *ca*. 96% of the Bodipy emission is quenched by the fullerene moiety. The bodipy dyes used as stoppers in **7** are not particularly strong electron donors neither in their ground nor excited states. The Bodipy singlet excited state in **7** is actually quenched by an efficient singlet-singlet energy transfer leading to the population of the first fullerene singlet excited state.

CONCLUSIONS

Porphyrins have been very useful building blocks for the functionalization of the pillar[5]arene and rotaxane scaffolds developed in our group. On one hand, the grafting of Zn(II)porphyrin subunits onto a clickable pillar[5]arene core has generated large multiporphyrinic arrays **1Zn$_{10}$** and **2Zn$_{10}$** in which weak interactions resulting from the intramolecular coordination of metalloporphyrin subunits with 1,2,3-triazole moieties are responsible for their partial folding. Interestingly, their degree of folding can be perfectly controlled by oxidation or reduction of the peripheral Zn(II)porphyrin groups. Upon oxidation, all the peripheral Zn(II)porphyrins are coordinated thus generating totally folded decacations. In contrast, their reduction disrupts the triazole-Zn(II) interactions and thus promotes a complete blooming of the molecular flowers. On the other hand, intriguing photoactive molecular devices have been constructed from pillar[5]arene-based rotaxane scaffolds. In such compounds (**3Zn$_{10}$(H$_2$)$_1$**, **6H$_2$** and **7**), complementary subunits are associated into a single molecular ensemble but without being connected through covalent bonds. Inter-component photo-induced energy transfer processes remain however extremely fast in these systems despite the exclusive link through mechanical bonds. These first examples of photoactive rotaxanes pave the way towards the preparation of new molecular machines in which the emission properties will be modulated by controlling the position of the pillar[5]arene subunit along its axle. Work in this direction is currently under way in our laboratories.

Acknowledgements

Financial support by the ANR (projects FastGiant ANR-17-CE07-0012-01 and Pillar ANR-19-CE06-0032), the *Fondation Jean-Marie Lehn* and the LabEx "Chimie des Systèmes Complexes" is gratefully acknowledged.

REFERENCES

1. Ogoshi T, Yamagishi T and Nakamoto Y. *Chem. Rev*. 2016; **116**: 7937-8002.
2. (a) Ogoshi T, Kitajima K, Aoki T, Fujinami S, Yamagishi T and Nakamoto Y. *J. Org. Chem*. 2010; **75**: 3268-3273. (b) Cao D, Kou Y, Liang J, Chen Z, Wang L and Meier H. *Angew. Chem. Int. Ed*. 2009; **48**: 9721-9724. (c) Holler M, Allenbach N, Sonet J and Nierengarten JF. *Chem. Commun*. 2012; **48**: 2576-2578.
3. Ogoshi T, Kanai S, Fujinami S, Yamagishi TA and Nakamoto Y. *J. Am. Chem. Soc*. 2008; **130**: 5022–5023.
4. (a) Zhang H and Zhao Y. *Chem. Eur. J*. 2013; **19**: 16862–16879. (b) Ogoshi T and Yamagishi T. *Eur. J. Org. Chem.* 2013: 2961-2975.
5. For selected recent reviews, see: (a) Li, Z and Yang YW. *Acc. Mater. Res.* 2021; **2**: 292-305. (b) Nierengarten I, Holler M, Rémy M, Hahn U, Billot A, Deschenaux R and Nierengarten JF. *Molecules* 2021; **26**: 2358. (c) Zhang H and Han J.

Org. Biomol. Chem. 2020; **26**: 4894-4905. (d) Kakuta T, Yamagishi T and Ogoshi T. *Acc. Chem. Res.* 2018; **51**: 1656-1666. (e) Zhang H, Liu Z and Zhao Y. *Chem. Soc. Rev.* 2018; **47**: 5491-5528.

6. (a) Nierengarten I, Buffet K, Holler M, Vincent SP and Nierengarten JF, *Tetrahedron Lett.* 2013; **54**: 2398-2402. (b) Vincent SP, Buffet K, Nierengarten I, Imberty A and Nierengarten JF. *Chem. Eur. J.* 2016*;* **22***:* 88-92. (c) Buffet K, Nierengarten I, Galanos N, Gillon E, Holler M, Imberty A, Matthews SE, Vidal S, Vincent SP and Nierengarten JF. *Chem. Eur. J.* 2016; **22**: 2955-2963. (d) Tikad A, Fu H, Sevrain CM, Laurent S, Nierengarten JF and Vincent SP, *Chem. Eur. J.* 2016; **22**: 13147-13155.
7. Nierengarten I, Nothisen M, Sigwalt D, Biellmann T, Holler M, Remy JS and Nierengarten JF. *Chem. Eur. J.* 2013; **19**: 17552-17558.
8. Bettucci O, Pascual J, Turren-Cruz SH, Cabrera-Espinoza A, Matsuda W, Völker SF, Köbler H, Nierengarten I, Reginato G, Collavini S, Seki S, Nierengarten JF, Abate A and Delgado JL. *Chem. Eur. J*. 2021; **27**: 8110-8117.
9. (a) Steffenhagen M, Latus A, Trinh TMN, Nierengarten I, Lucas IT, Joiret S, Landoulsi J, Delavaux-Nicot B, Nierengarten JF and Maisonhaute E. *Chem. Eur. J*. 2018; **24**: 1701-1708. (b) Boitel-Aullen G, Fillaud L, Huet F, Nierengarten I, Delavaux-Nicot B, Nierengarten JF and Maisonhaute E. *ChemElectroChem* 2021; **8**: 3506-3511.
10. (a) Nierengarten I, Guerra S, Holler M, Nierengarten JF and Deschenaux R. *Chem. Commun*. 2012; **48**: 8072-8074. (b) Nierengarten I, Guerra S, Holler M, Karmazin-Brelot L, Barberá J, Deschenaux R and Nierengarten JF. *Eur. J. Org. Chem*. 2013: 3675-3684. (c) Nierengarten I, Guerra S, Ben Aziza H, Holler M, Abidi R, Barberá J, Deschenaux R and Nierengarten JF. *Chem. Eur. J.* 2016; **22**: 6185-6189.
11. Kardelis V, Li K, Nierengarten I, Holler M, Nierengarten JF and Adronov A. *Macromolecules* 2017; **50**: 9144-9150.
12. (a) Milev R, Lopez-Pacheco A, Nierengarten I, Trinh TMN, Holler M, Deschenaux R and Nierengarten JF. *Eur. J. Org. Chem*. 2015: 479-485. (b) Trinh TMN, Nierengarten I, Holler M, Gallani JL and Nierengarten JF. *Chem. Eur. J*. 2015; **21**: 8019-8022. (c) Nierengarten I, Meichsner E, Holler M, Pieper P, Deschenaux R, Delavaux-Nicot B and Nierengarten JF. *Chem. Eur. J*. 2018; **24**: 169-177. (d) Holler M, Stoerkler T, Louis A, Fisher F and Nierengarten JF. *Eur. J. Org. Chem*. 2019: 3401-3405. (e) Nierengarten I and Nierengarten JF. *ChemistryOpen* 2020; **9**: 393-400.
13. (a) Mateo-Alonso A, Sooambar C and Prato M. *C. R. Chim.* 2006; **9**: 944–951. (b) D'Souza F and Ito O. *Chem. Commun.* 2009: 4913-4928. (c) Nierengarten JF. *Eur. J. Inorg. Chem*. 2019: 4865-4878.
14. Maeda C, Yamaguchi S, Ikeda C, Shinokubo H and Osuka A. *Org. Lett.* 2008; **10**: 549-552.
15. Nguyen NT, Mamardashvili GM, Kulikova OM, Scheblykin IG, Mamardashvili NZ and Dehaen W. *RSC Adv*. 2014; **4**: 19703-19709.
16. (a) Collin JP, Durola F, Heitz V, Reviriego F, Sauvage JP and Trolez Y. *Angew. Chem. Int. Ed*. 2010; **49**: 10172-10175. (b) Tse YC, Hein R, Mitchell EJ, Zhang Z and Beer PD. *Chem. Eur. J.* 2021; **27**: 14550-14559. (c) Wolf M, Ogawa A, Bechtold M, Vonesch M, Wytko JA, Oohora K, Campidelli S, Hayashi T, Guldi DM and Weiss J. *Chem. Sci.* 2019; **10**: 3846-3853. (d) Miyazaki Y, Kahlfuss C, Ogawa A, Matsumoto T, Wytko JA, Oohora K, Hayashi T and Weiss J. *Chem. Eur. J.* 2017; **23**: 13579-13582. (e) Roberts DA, Schmidt TW, Crossley MJ and Perrier S. *Chem. Eur. J.* 2013; **19**: 12759-12770.
17. Lõkov M, Tshepelevitsh S, Heering A, Plieger PG, Vianello R, and Leito I. *Eur. J. Org. Chem*. 2017: 4475-4489.
18. Maeda C, Kim P, Cho S, Park JK, Lim JM, Kim D, Vura-Weis J, Wasielewski MR, Shinokubo H and Osuka A. *Chem. Eur. J.* 2010; **16**: 5052-5061.
19. Trinh TMN, Nierengarten I, Ben Aziza H, Meichsner E, Holler M, Chessé M, Abidi R, Bijani C, Coppel Y, Maisonhaute

E, Delavaux-Nicot B and Nierengarten JF. *Chem. Eur. J.* 2017; **23**: 11011-11021.

20. Delavaux-Nicot B, Ben Aziza H, Nierengarten I, Trinh TMN, Meichsner E, Chessé M, Holler M, Abidi R, Maisonhaute E and Nierengarten JF. *Chem. Eur. J*. 2018; **24**: 133-140.
21. Linke M, Chambron JC, Heitz V, Sauvage JP, Encinas S, Barigelletti F and Flamigni L. *J. Am. Chem. Soc.* 2000; **122**: 11834-11844.
22. Meichsner E, Nierengarten I, Holler M, Chessé M and Nierengarten JF. *Helv. Chim. Acta* 2018; **101**: e1800059.
23. Rémy M, Nierengarten I, Park B, Holler M, Hahn U and Nierengarten JF. *Chem. Eur. J*. 2021; **27**: 8492-8499.
24. (a) Imahori H and Sakata Y. *Eur. J. Org. Chem.* 1999: 2445–2457. (b) Gust D, Moore TA and Moore AL. *Acc. Chem. Res.* 2001; **34**: 40–48. (c) Guldi DM. *Chem. Soc. Rev.* 2002; **31**: 22–36.

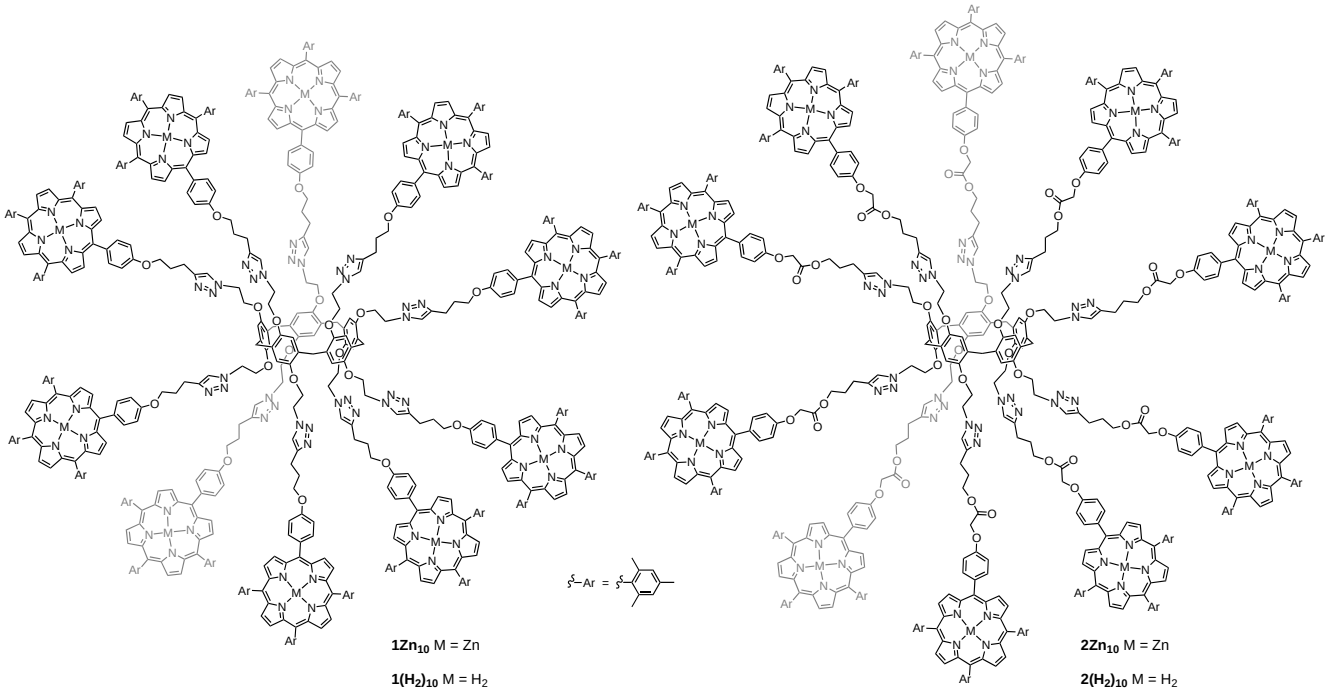

Figure 1. Multi-Zn(II)porphyrin arrays **1Zn$_{10}$** and **2Zn$_{10}$** as well as the corresponding free-base derivatives **1(H$_2$)$_{10}$** and **2(H$_2$)$_{10}$**.

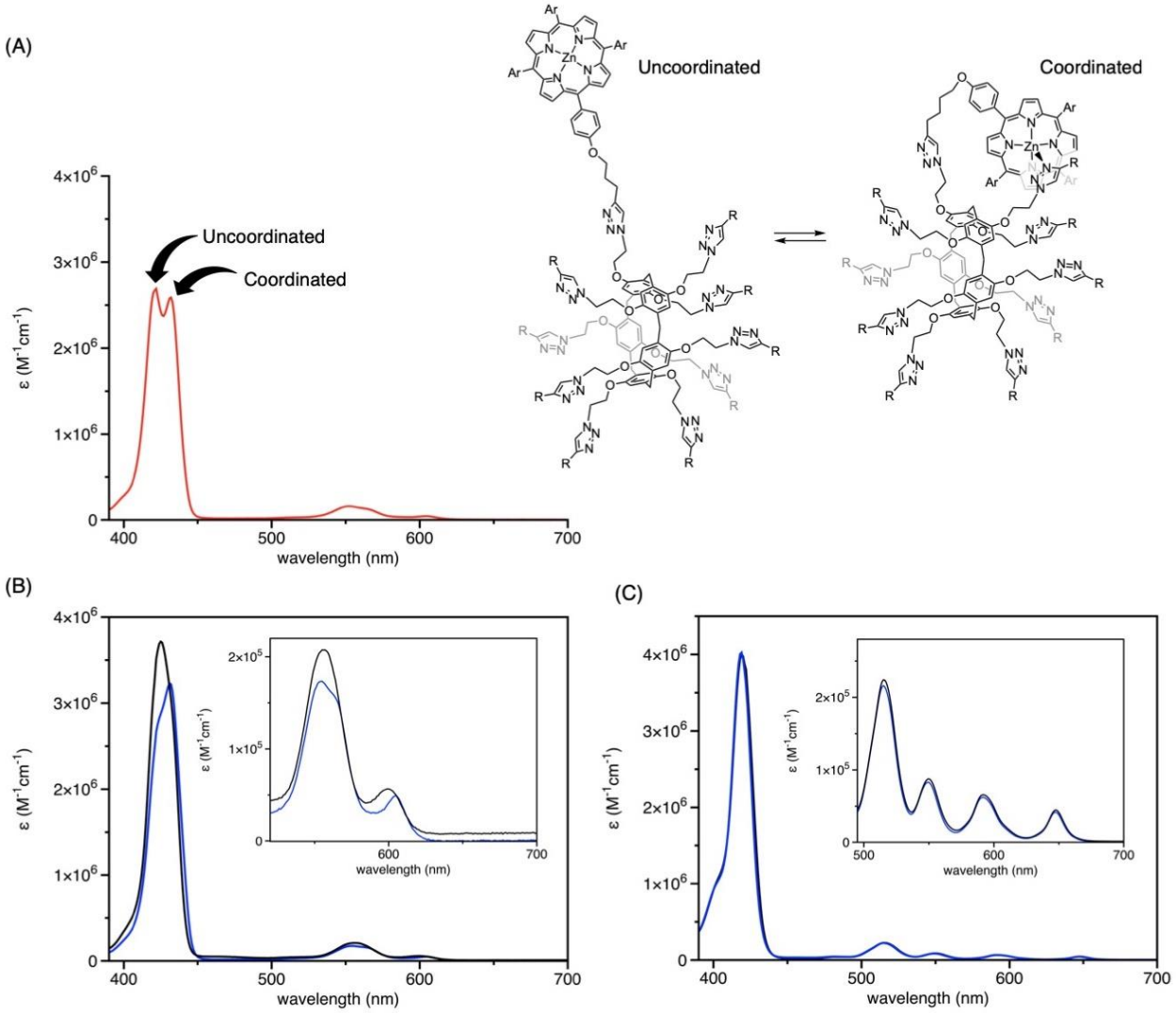

Figure 2. (A) Absorption spectrum of compound **1Zn$_{10}$** recorded in CH_2Cl_2 at 25°C and schematic representation of the dynamic conformational equilibrium resulting from the intramolecular coordination of a 1,2,3-triazole moiety to a Zn(II)porphyrin subunit in **1Zn$_{10}$**. (B) Absorption spectra of compound **1Zn$_{10}$** recorded in PhMe (blue) and $CHCl_3$ (black) at 25°C. (C) Absorption spectra of compounds **1(H$_2$)$_{10}$** (black) and **2(H$_2$)$_{10}$** (blue) recorded in CH_2Cl_2 at 25°C.

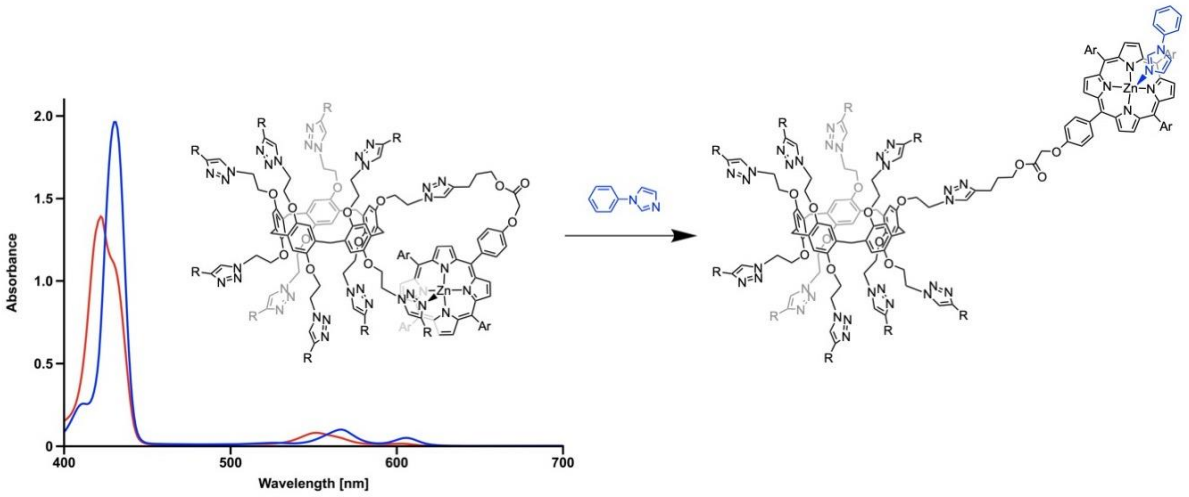

Figure 3. Absorption spectra of compound **2Zn$_{10}$** before (red) and after (blue) addition of 1-phenylimidazole (14 equiv.) recorded in CH_2Cl_2 at 25°C and schematic representation of the blooming of molecular flower **2Zn$_{10}$** upon addition of 1-phenylimidazole.

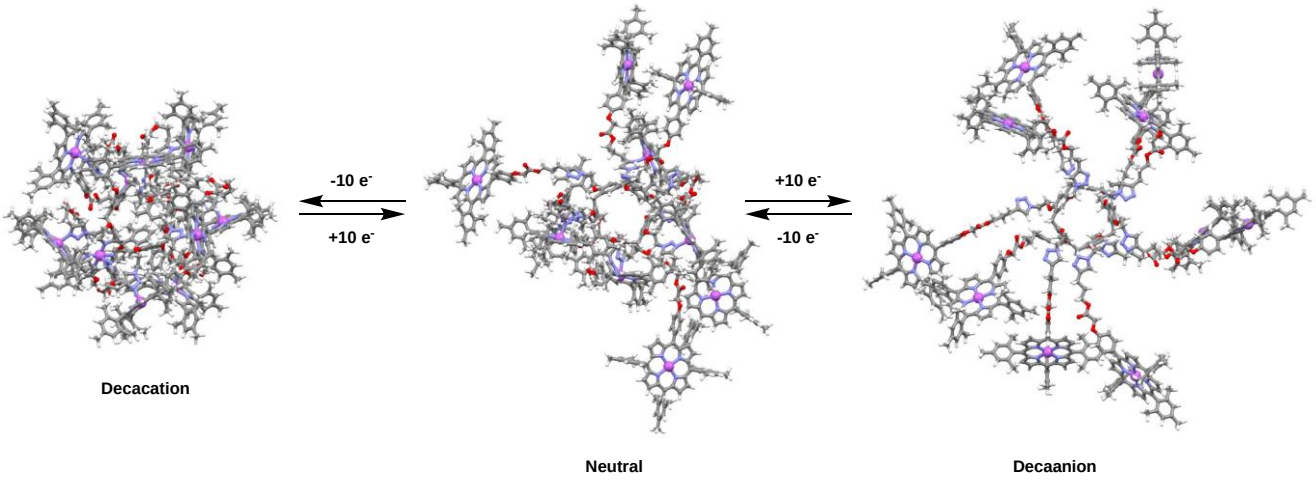

Figure 4. Schematic representation of the electrochemically triggered conformational changes of compound **2Zn$_{10}$** based on calculated structures.

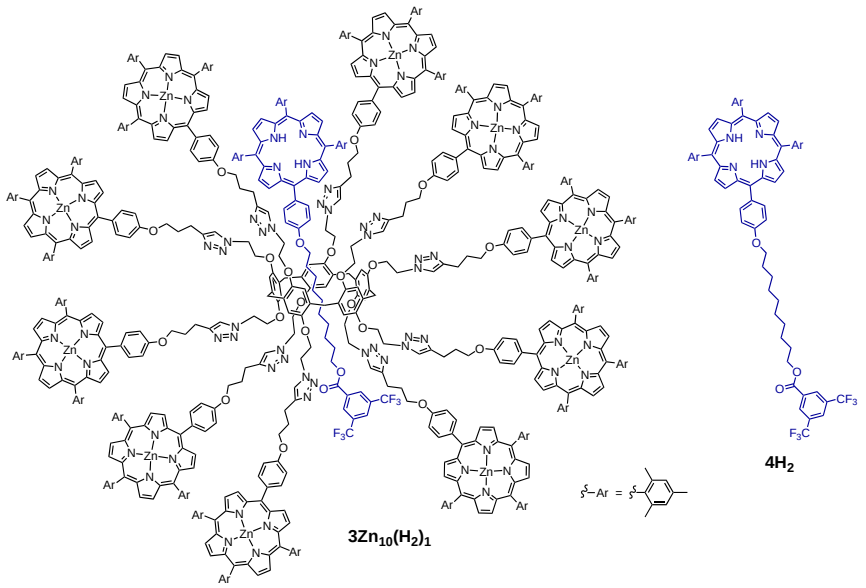

Figure 5. Light harvesting device $\mathbf{3Zn_{10}(H_2)_1}$ and free-base porphyrin model compound $\mathbf{4H_2}$.

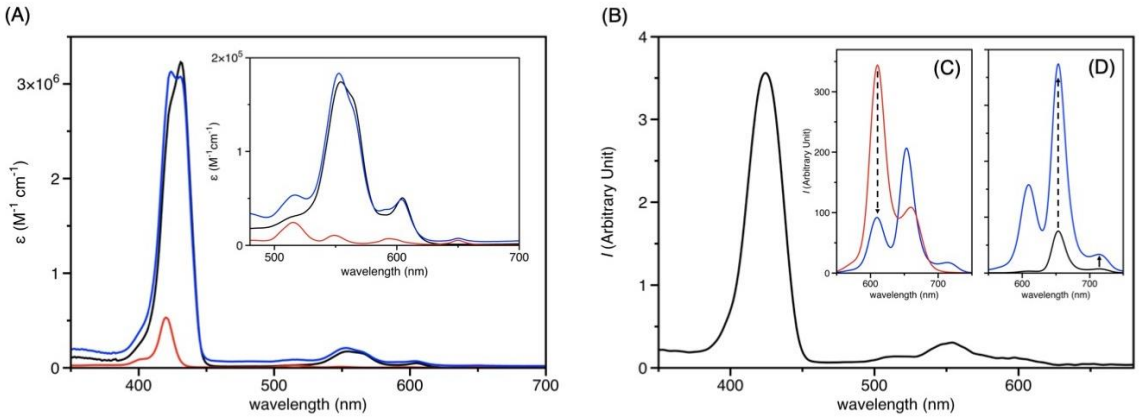

Figure 6. (A) Absorption spectra of compounds $\mathbf{4H_2}$ (red), $\mathbf{1Zn_{10}}$ (black) and $\mathbf{3Zn_{10}(H_2)_1}$ (blue) recorded in PhMe at 25°C. (B) Excitation spectrum recorded for compound $\mathbf{3Zn_{10}(H_2)_1}$ in PhMe (λ_{em} = 720 nm). (C) Emission spectra of isoabsorbing solutions of compounds $\mathbf{1Zn_{10}}$ (red) and $\mathbf{3Zn_{10}(H_2)_1}$ (blue) in PhMe (25°C, λ_{exc} = 425 nm). (D) Emission spectra of compounds $\mathbf{4H_2}$ (black) and $\mathbf{3Zn_{10}(H_2)_1}$ (blue) in PhMe (25°C, λ_{exc} = 425 nm), the concentration of the two solutions are identical.

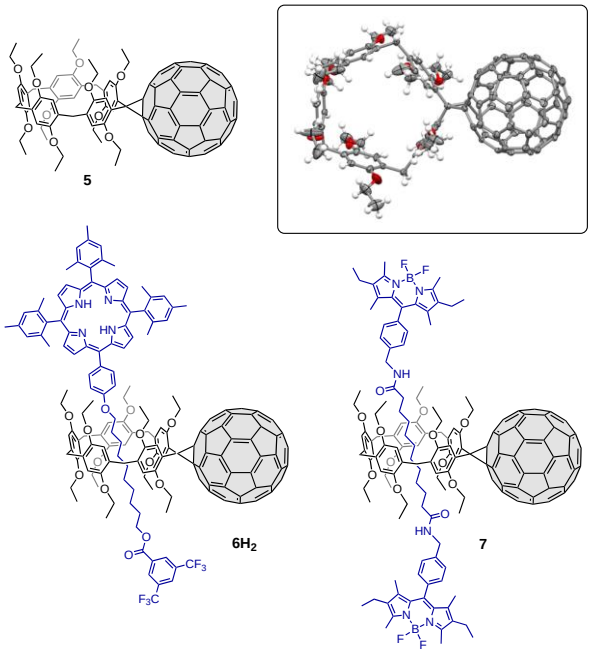

Figure 7. Fulleropillar[5]arene **5** and photoactive [2]rotaxanes **6H₂** and **7**. Inset: ORTEP plot of the structure of **5** (C: gray, O: red, H: white; thermal ellipsoids are shown at the 30% probability level).

Pillar[5]arene-porphyrin conjugates: from molecular flowers to photoactive rotaxanes

Iwona Nierengarten, Uwe Hahn, Michel Holler, Béatrice Delavaux-Nicot, Emmanuel Maisonhaute and Jean-François Nierengarten

The combination of porphyrin derivatives with our pillar[5]arene-containing building blocks attracted our attention for the preparation of photo- and/or electro-active molecular devices. This aspect of our research program on functionalized pillar[5]arene derivatives is summarized in the present account.